THE JOURNAL OF PHYSICAL CHEMISTRY B

Article

pubs.acs.org/JPCB

Ultrafast Librational Relaxation of H_2O in Liquid Water

Jakob Petersen,[†] Klaus B. Møller,*[,†] Rossend Rey,*[,‡] and James T. Hynes*[,§,∥]

[†]Department of Chemistry, Technical University of Denmark, 2800 Kgs. Lyngby, Denmark

[‡]Departament de Física i Enginyeria Nuclear, Universitat Politècnica de Catalunya, Barcelona 08034, Spain

[§]Department of Chemistry and Biochemistry, University of Colorado, Boulder, Colorado 80309-0215, United States

[∥]Chemistry Department, Ecole Normale Supèrieure, UMR ENS-CNRS-UPMC 8640, 24 Rue Lhomond, 75005 Paris, France

Supporting Information

ABSTRACT: The ultrafast librational (hindered rotational) relaxation of a rotationally excited H_2O molecule in pure liquid water is investigated by means of classical nonequilibrium molecular dynamics simulations and a power and work analysis. This analysis allows the mechanism of the energy transfer from the excited H_2O to its water neighbors, which occurs on a sub-100 fs time scale, to be followed in molecular detail, i.e., to determine which water molecules receive the energy and in which degrees of freedom. It is found that the dominant energy flow is to the four hydrogen-bonded water partners in the first hydration shell, dominated by those partners' rotational motion, in a fairly symmetric fashion over the hydration shell. The minority component of the energy transfer, to these neighboring waters' translational motion, exhibits an asymmetry in energy reception between hydrogen-bond-donating and -accepting water molecules. The variation of the energy flow characteristics with rotational axis, initial rotational energy excitation magnitude, method of excitation, and temperature is discussed. Finally, the relation of the nonequilibrium results to equilibrium time correlations is investigated.

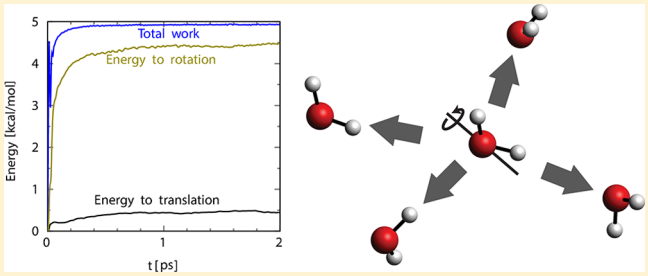

1. INTRODUCTION

The dynamics of the librations (hindered rotations) of liquid water are not well understood, despite their invocation as (a) important energy receptors in the pathways for energy relaxation of the water stretch and bend vibrational excitations[1−13] and of some solute vibrations in aqueous solutions,[14,15] (b) essential participants in the rearrangements of the hydrogen bond networks of water and aqueous solutions,[16,17] and (c) ingredients in various reactive processes, one example being nonadiabatic transitions for the hydrated electron.[18,19] In the present work, we investigate some key aspects of water librational dynamics. In particular, we examine, via classical nonequilibrium molecular dynamics simulations and a work and power formulation of energy transfer, the relaxation time scale and molecular level energy transfer pathway of a rotationally excited water molecule in water.

Much of the explicit scrutiny of pure liquid water libration dynamics is fairly recent and concerned with vibrational energy relaxation. Librational excitations in liquid water have been experimentally studied via femtosecond two-color infrared spectroscopy,[1−3] both directly and in connection with the energy transfer from excited water bend vibration. For direct librational excitation, the relaxation time scale is extremely short: sub-100 fs.[1−3] In connection with water bend excitation, librations were invoked as the major initial recipient of the excess water bend energy.[1−3] On the theoretical side, in this last connection, several of us and co-workers have studied the bend relaxation mechanism.[4−6] This was shown,[5] via a power and work analysis,[14,20−23] to primarily involve a centrifugal coupling 2:1 Fermi resonance intramolecular energy transfer route from the bend to water rotation, leading to subsequent flow, primarily to water librations in the first and second hydration shells of the initially bend-excited water molecule.[5] A very recent Poisson bracket reformulation[6] of the power and work description allowed the explicit identification of *which* water molecules (e.g., first hydration shell water accepting a hydrogen bond from the excited water) and degrees of freedom (rotation, translation) are key in accepting the energy.

In the present work, we apply the power and work formulation, in its Poisson bracket formulation, to the energy flow mechanism for a directly rotationally excited water molecule, a process which has not received much previous theoretical attention, primarily due to the comparatively limited experimental scrutiny noted above.[1−3] Prior theoretical work here includes those of nonequilibrium excited water rotation by Ingrosso et al.[4] and to a more restricted degree (in connection with water bend relaxation) by Rey et al.,[5] as well as by Saito and co-workers.[24−26] These last authors initially focused on 2D infrared spectroscopy[24,25] and more recently[26] on a combination of nonequilibrium simulations and kinetic equation

Special Issue: Paul F. Barbara Memorial Issue

Received: August 31, 2012
Revised: October 31, 2012
Published: November 6, 2012

   dx.doi.org/10.1021/jp308648u | *J. Phys. Chem. B* 2013, 117, 4541−4552

modeling in a way complementary to ours, to be discussed within. The present study extends the initial study of this process by Ingrosso et al.[4] (which did not exploit a power-work approach) in a number of important ways. First and foremost, the specific identity of energy-accepting water molecules and degrees of freedom is found. In addition, a wider range of rotational excitation energies, temperatures, and rotational axes is examined, and excitation via an external electric field is considered in addition to instantaneous excitation via an initial assignment of excess rotational energy. Further, an extensive comparison of the nonequilibrium results with a linear response perspective is given.

The outline of the remainder of this paper is as follows. The basic theoretical power-work formulation is presented in section 2, while section 3 is concerned with various computational details. Section 4 presents and discusses the simulation results (with some details provided as Supporting Information), followed by concluding remarks offered in section 5. Two Appendices deal, respectively, with an alternative derivation of the key power-work relationships and with the connection of the nonequilibrium relaxation dynamics to equilibrium fluctuations.

2. THEORETICAL BACKGROUND

The work on the rotationally excited H_2O molecule done by the surrounding water molecules proves to be a very useful quantity for examining the energy flow during the librational relaxation. This work is the time-integrated power associated with the rotational kinetic energy of the central water molecule, and the elaboration of that power provides considerable information on the energy flow mechanism and time scale.

Before proceeding, we pause to make several brief remarks concerning nomenclature. First, any rotation of a water molecule in the liquid is of course hindered, i.e., librational in character. Since we will be primarily concerned with rotational kinetic energy and a "libration" actually refers to both kinetic and potential energy aspects, hereafter we will generally employ the terms "rotation" or "rotational", while occasionally using "libration" or "librational" in a more loose sense. It is also relevant to remark that the current absence of the knowledge of librational modes' in liquid water dictates a focus on the rotational kinetic energy.[4] Finally, for economy of expression, we will often refer to the rotationally excited H_2O molecule as the "central molecule" and the water molecules surrounding this central molecule as "the solvent".

In the ensuing analysis, we apply the analysis of power and work contributions used previously by Whitnell, Wilson, and Hynes.[14,15] A general discussion of the power-work formalism for energy relaxation, particularly in a Poisson bracket formulation we employ here, can be found in ref 6 (and in Appendix A we offer an alternative derivation of the formulas employed within). We begin the theoretical development by writing the Hamiltonian for a set of rigid water molecules in which the rotational kinetic energy of one of them (R_i) is singled out

$$H = R_i + U + H' \tag{1}$$

where U denotes the coupling between molecule i and its neighbors and H' contains the rest of the Hamiltonian's contributions including the translational kinetic energy of molecule i (i.e., $H' = T_i + H_{\text{rest}}$).

The time variation of the rotational kinetic energy R_i—the power associated with this energy—can be expressed in terms of Poisson brackets as

$$\frac{dR_i}{dt} = [R_i, H] = [R_i, U] \tag{2}$$

an expression which results in

$$\frac{dR_i}{dt} = [R_i, U] = -\frac{\partial R_i}{\partial \mathbf{p}_{\alpha_i}}\cdot\frac{\partial U}{\partial \mathbf{r}_{\alpha_i}} = (\boldsymbol{\omega}_i \times \mathbf{r}_{\alpha_i})\cdot\mathbf{F}_{\alpha_i} = \boldsymbol{\omega}_i\cdot\boldsymbol{\tau}_i \tag{3}$$

where $\{\mathbf{r}_{\alpha_i}\}$ and $\{\mathbf{p}_{\alpha_i}\}$ denote the position and momentum vectors of the excited molecule's atoms, and the summation over repeated indexes convention has been adopted; see ref 6. This is of course the well-known angular velocity ($\boldsymbol{\omega}_i$) times torque ($\boldsymbol{\tau}_i$) formula, which identifies the work that each of the neighbors exerts on rotation of molecule i.

We are interested however in identifying the energy-accepting molecules and degrees of freedom in the energy transfer mediated by the interaction energy U. The latter's time variation can be expressed in a fashion similar to that of rotational kinetic energy as

$$\frac{dU}{dt} = [U, H] = [U, R_i] + [U, H'] = [U, R_i] + [U, T_i] + [U, H_{\text{rest}}] \tag{4}$$

which, when inserted in place of the rightmost term in eq 2, results in

$$\frac{dR_i}{dt} = -\frac{dU}{dt} + [U, T_i] + [U, H_{\text{rest}}] \tag{5}$$

By identifying the second term on the right-hand side of eq 5 as the time derivative of the translational kinetic energy of molecule i and expressing H_{rest} in terms of the Cartesian coordinates $\{\mathbf{r}_{\beta_i}\}$ of the constituent atoms, we can write

$$\frac{dR_i}{dt} = -\frac{dU}{dt} - \frac{dT_i}{dt} + \frac{\partial U}{\partial \mathbf{r}_{\beta_j}}\cdot\frac{\partial H_{\text{rest}}}{\partial \mathbf{p}_{\beta_j}} = -\frac{dU}{dt} - \frac{dT_i}{dt} - \mathbf{F}_{\beta_j,i}\cdot\mathbf{v}_{\beta_j} \tag{6}$$

where the forces are exerted by molecule i. Finally, considering that $\mathbf{v}_{\beta_j} = \mathbf{v}_j + \boldsymbol{\omega}_j \times \mathbf{r}_{\beta_j}$, where $\mathbf{v}_j$ is the center of mass velocity of molecule j, $\boldsymbol{\omega}_j$ is the angular velocity of molecule j, and $\mathbf{r}_{\beta_j}$ is the position of atom β_j with respect to the center of mass of molecule j, we obtain an expression for the power of the rotational kinetic energy of the ith molecule

$$\frac{dR_i}{dt} = -\frac{dU}{dt} - \frac{dT_i}{dt} - \sum_{j\neq i}\mathbf{F}_{j,i}\cdot\mathbf{v}_j - \sum_{j\neq i}\boldsymbol{\tau}_{j,i}\cdot\boldsymbol{\omega}_j \tag{7}$$

involving the summation over molecule i's neighboring molecules.

The first term in this rotational power in eq 7 is the contribution to the power from the interaction potential energy between the central molecule and the solvent, the second and third terms are the translational kinetic energy contributions from the central excited water molecule and the surrounding

dx.doi.org/10.1021/jp308648u | J. Phys. Chem. B 2013, 117, 4541−4552

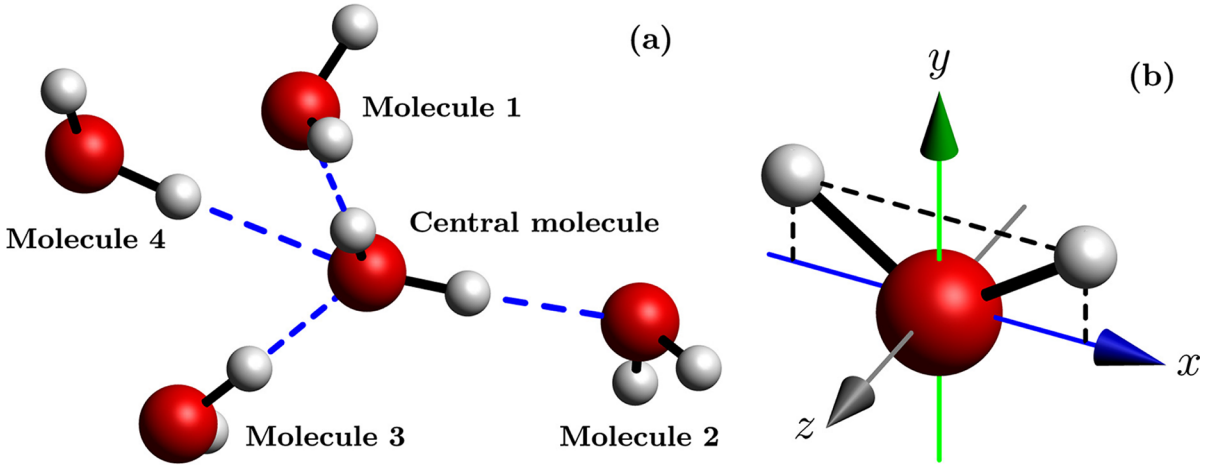

Figure 1. (a) The central water molecule is hydrogen-bonded to four water molecules in its first hydration shell. Molecules 1 and 2 are accepting H-bonds from the central H_2O molecule, and molecules 3 and 4 are donating H-bonds to the central molecule. (b) The principal axes for a rigid H_2O molecule. The corresponding moments of inertia are $I_{xx} \cong 0.6$, $I_{yy} \cong 1.3$, and $I_{zz} \cong 1.9$ (in amu·Å^2).[5]

water solvent, respectively, and the fourth term is the rotational kinetic energy contribution from the solvent.

If we now set i = C to conveniently label the central molecule, the work corresponding to this rotational power is defined by

$$W_C(t) \equiv \int_{t_0}^{t} dt' \frac{dR_C}{dt'} = \Delta R_C \tag{8}$$

where $W_C(t)$ denotes the difference in rotational kinetic energy of the central molecule between time t_0 and t, i.e., the transfer of the excited water's excess rotational kinetic energy to the surrounding solvent molecules. With the aid of eq 7, our final expression for the rotational work is

$$W_C = -\Delta U - \Delta T_C - W_T - W_R \tag{9}$$

in which the explicit expressions for the work terms are

$$W_T(t) = \int_{t_0}^{t} dt' \sum_{j \neq C} \mathbf{F}_{j,C}(t') \cdot \mathbf{v}_j(t') \tag{10}$$

$$W_R(t) = \int_{t_0}^{t} dt' \sum_{j \neq C} \boldsymbol{\tau}_{j,C}(t') \cdot \boldsymbol{\omega}_j(t') \tag{11}$$

We summarize the meaning of the terms on the right-hand side in the key result eq 9. The first term is the difference in potential energy (due to interactions between the central water molecule and the surrounding solvent waters) between time t_0 and t, the second term is the change in translational kinetic energy of the central molecule, and the third and fourth terms are the energy transferred to the translational and rotational degrees of freedom of the surrounding water solvent. Hence—and this is the key point—we can determine to which molecules and degrees of freedom of the surrounding water solvent the excited water molecule's excess rotational kinetic energy is transferred.

Finally, in order to obtain a detailed molecular picture of the pathway of the energy flow, we divide the solvent into hydration shells around the central excited water molecule. The first shell corresponds to the four nearest water molecules, where two of these are accepting hydrogen (H)-bonds from the central water and two are donating H-bonds, as illustrated in Figure 1a. The second shell consists of all water molecules, except the four nearest, within a radial distance of ∼5.7 Å with respect to the central molecule. Under equilibrium conditions at $T \approx 300$ K, the second shell includes 21.6 molecules on average.

3. COMPUTATIONAL METHODS

Addressing first some general computational issues, the classical MD simulations are carried out with an in-house code, which applies cubic periodic boundary conditions and the minimum image convention for a system of 216 H_2O molecules. The atomic equations of motion are solved with the velocity-Verlet algorithm using a time step of 0.5 fs, and the intermolecular forces are described by the SPC/E model.[27,28] The length of the simulation box is $L \approx 18.6$ Å corresponding to the experimental value of the density ($\rho = 0.998$ g/cm^3) at $T \approx 300$ K,[29] and the cutoff distance is $L/2$. The Ewald summation correction for the Coulomb forces has been included with $\alpha = 5L$ and $n_{max}^2 = 25$.[30] The water molecules are kept rigid during the simulations with the RATTLE algorithm[31] (with a relative accuracy of 10^{-7}), and the Nosé–Hoover thermostat[32] is used for the initial thermal equilibration.

3.1. Initial Conditions. In order to obtain a statistical picture of the librational relaxation process, a set of equilibrated initial conditions of the system is produced. The setup of the simulation box corresponds to a simple cubic lattice with a water molecule at each lattice point, and the orientations of the molecules are the same. The molecular linear and angular velocities are chosen from Maxwell–Boltzmann distributions at $T = 300$ K.[33] This setup corresponds to a very repulsive state, and the temperature increases significantly within 2 ps of the propagation. The Nosé–Hoover thermostat is turned on to correct for the increase in the temperature, and after 500 ps, the system is equilibrated at $T \approx 300$ K. The thermostat is then turned off, and the propagation is continued under *NVE* conditions for 100 ps.

A total number of 20 000 initial conditions is produced from a 100 ns *NVE* simulation run, where snapshots of phase space points are saved every 5 ps. After the atomic positions and velocities are saved, new random molecular linear and angular velocities at $T = 300$ K are chosen for each molecule. With this procedure, the initial conditions correspond to a canonical ensemble at $T \approx 300$ K with a standard deviation of ∼9 K.

dx.doi.org/10.1021/jp308648u | J. Phys. Chem. B 2013, 117, 4541−4552

Similar procedures are followed for the other temperatures examined.[34]

These considerations suffice for, e.g., equilibrium time correlation function calculations. We now turn to the special features associated with nonequilibrium simulations.

3.2. Nonequilibrium MD Simulations. Nonequilibrium MD (NEMD) simulations are carried out with instantaneous rotational excitations of the central water molecule. We commence with, and focus most attention on, the case where an energy of E_{rot} = 5 kcal/mol is added to the rotation with respect to the principal x-axis of the central molecule.

We pause to note that this rotational excitation energy choice corresponds to approximately one H_2O bend quantum of excitation.[4] This value is of interest in connection with the bend relaxation problem and is also useful in helping to make more visible various aspects of the energy flow. In order to investigate if the librational relaxation is dependent on the rotational excitation energy value of 5 kcal/mol, we carry out simulations where the excitation energy is varied from 1 to 15 kcal/mol. Special attention is also given to the 1 kcal/mol case as an illustration of rotational excitation in the thermal range.

Returning to the main thread, the angular velocity component corresponding to the excitation is found via $\omega_x = (2E_{rot}/I_{xx})^{1/2}$, where I_{xx} is the principal moment of inertia element associated with the x-axis. The value of ω_x is added to the existing value of the angular velocity component, which can be both negative and positive. Hence, the initial rotational energy of the central molecule is not equal to, for example, 5 kcal/mol (plus the equilibrium value) for each trajectory but can be both less than or greater than 5 kcal/mol (plus the equilibrium value). However, on average, the excitation energy is 5 kcal/mol. (This prescription differs from that of ref 4.)[35] The system is then propagated until the rotational relaxation of the excited water molecule is completed. The same calculations are carried out for separate excitations with respect to the principal y- and z-axes, shown in Figure 1b.

The librational energy relaxation is found to proceed very rapidly, and it is possible that the width of an experimental optical excitation pulse might influence the decay time. In order to examine this issue, the rotational excitation is also carried out via an external time-dependent electric field; the details of these simulations are best presented, together with the results, in section 4.5.

Finally, the NEMD simulations were checked for finite-size effects by comparing results for a system of 64 H_2O molecules with those for systems of 216 and 343 H_2O molecules, respectively. The librational energy decay shows no significant difference for the three systems, and we base all the presented MD simulation results on the 216 H_2O molecule system.

4. SIMULATION RESULTS AND DISCUSSION

4.1. Rotational Kinetic Energy Relaxation. We begin with simulation results for the decay to equilibrium of the rotational kinetic energy for the initially rotationally excited central water molecule. Figure 2a displays several examples of the time dependence of the rotational kinetic energy (of 5 kcal/mol) of the central molecule for three of the NEMD trajectories in which the instantaneous rotational excitation is with respect to the principal x-axis. These different trajectory results give an impression, first, of the differing initial rotational energies as explained in section 3.2 and, second, of an oscillatory character, at least for the shortest times where there is a qualitative agreement for all three trajectories. Such

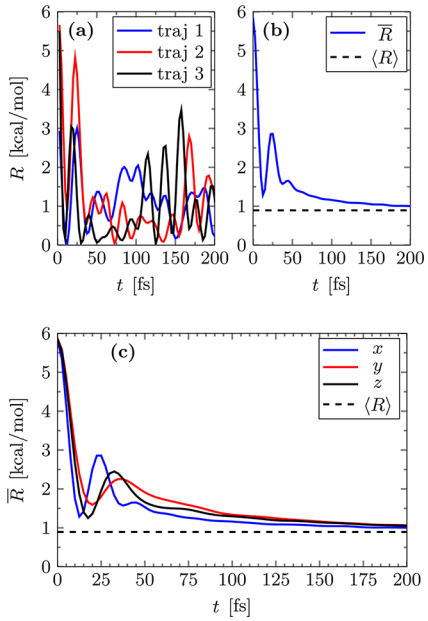

Figure 2. (a) The nonequilibrium rotational kinetic energy R of the central water molecule as a function of time for instantaneous 5 kcal/mol rotational excitation with respect to the principal x-axis (for three of the NEMD trajectories) and (b) the corresponding nonequilibrium average rotational kinetic energy $\overline{R}$ based on 20 000 NEMD trajectories. The equilibrium average rotational kinetic energy $\langle R \rangle \approx 0.894$ kcal/mol $(3N_A k_B T/2)$ is also shown. (c) The nonequilibrium average rotational kinetic energy $\overline{R}$ of the central water molecule as a function of time for 5 kcal/mol rotational excitation with respect to the principal x-, y-, and z-axes. A similar figure was reported by Ingrosso et al.[4]

an oscillatory aspect of energy relaxation, first observed for water rotation in ref 4, is unusual.

The average rotational kinetic energy of the central water molecule based on 20 000 NEMD trajectories is shown in Figure 2b. The first point of importance is that the main portion of the excitation energy is lost within ~100 fs, which agrees with the decay behavior for librational excitation obtained by ultrafast IR experiments,[3] and earlier simulations.[4] Second, a single oscillation remains in this average decay. The local maximum in the rotational kinetic energy at $t \sim 25$ fs associated with this oscillation indicates clearly that most, if not all, NEMD trajectories are qualitatively quite similar with respect to the time evolution of the rotational kinetic energy during the first ~25 fs after the excitation, and that some degree of rotational coherence is maintained during that time interval. This initial oscillation in the average rotational kinetic energy decay is associated with rotational caging, in which the angular momentum is reversed due to the restraining torques exerted by the surrounding water molecules. This is established in Appendix B, which extends and generalizes the similar identification made for the total angular momentum in ref 4. Finally, we connect the oscillation with the librational spectrum in section 4.5.

The behavior just discussed is not restricted to the rotational excitation with respect to the principal x-axis. Figure 2c shows the excited water molecule's rotational kinetic energy as a function of time for excitation with respect to the principal x-, y-, and z-axes. The time evolutions are quite similar: the rotational kinetic energy drops from ~6 to ~1.5 kcal/mol within ~15 fs. Then, this energy increases to ~2.5 kcal/mol

dx.doi.org/10.1021/jp308648u | J. Phys. Chem. B 2013, 117, 4541−4552

within the next ∼15 fs in the course of the rotational caging oscillation, and completes the remaining small decline to the equilibrium value within ∼200 fs. In view of this similarity, we focus in the following on the results for the principal *x*-axis rotational excitation, and refer to the other axes results for particular points of interest.[36]

4.2. Work Analysis. We now proceed to apply the tools developed in section 2 to the analysis of the energy fluxes that characterize this process. The various terms in eq 9 for the work on the excited water molecule rotation, which are defined in detail below that equation, are plotted as functions of time in Figure 3. The main aspect to note from this plot is that, after 2

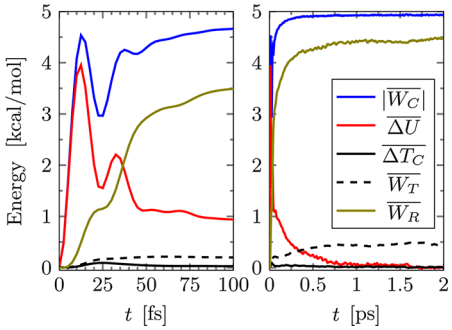

Figure 3. Nonequilibrium average work and energy terms for 5 kcal/mol rotational excitation of the central water molecule with respect to the principal *x*-axis. Shown are the absolute value of the work on the rotational degrees of freedom $|\overline{W_C}|$ of the central rotationally excited water molecule (equal to the magnitude of the molecule's energy loss), the difference in potential energy $\overline{\Delta U}$ between time 0 and *t*, the difference in translational kinetic energy $\overline{\Delta T_C}$ of the central water molecule, and the work on the translational $\overline{W_T}$ and rotational degrees of freedom $\overline{W_R}$ of the surrounding water solvent.

ps (and, to a significant degree, already established within ∼200 fs), ∼90% of the excitation energy has been transferred to the rotational degrees of freedom of the surrounding water molecules (as indicated by $\overline{W_R}$), and the remaining ∼10% is transferred to their translational degrees of freedom (as indicated by $\overline{W_T}$); the *y*- and *z*-axis excitation results are somewhat similar, with slightly more than ∼15% transfer to translation (see Table 1). Such overwhelming dominance of transfer of excess rotational kinetic energy to water solvent rotation is a key result of this work and is a natural consequence of the central molecule's rotational frequency being part of water's librational spectrum (∼400−800 cm^{-1}, see also Figure 6), whereas the translational spectrum lies at much lower frequencies ($\lesssim$200 cm^{-1}).[37] It stands in good agreement with the qualitative results reported for energy transfer from directly excited water rotation found by Ingrosso et al.[4] It is also consistent with the results found for bend energy relaxation, studied by Rey and Hynes with tools similar to the ones used here.[6] In this case, it was found that 94% of the initial vibrational excess energy goes into rotational motion, i.e, even higher proportion. This is to be expected given that the higher frequency associated with the bending motion is more off resonance (as opposed to rotation) with the low frequency characteristic of translation. An interesting aspect of all these results is that they show that loss of the initial excess energy, although being extremely fast, proceeds through a somewhat inefficient, i.e., indirect, equilibration between rotational and translational energy, suggesting a faster partial equilibration

Table 1. Work Contributions in Percentages at Time *t* = 2 ps[a]

	x-axis	*y*-axis	*z*-axis	I_0[b]
$\overline{W_R}$ (%)	91	82	84	91
$\overline{W_T}$ (%)	9	17	16	9
$\overline{\Delta U}$ (%)	0	1	0	0
$\overline{W_{C_{1st/2nd}}}$[c] (%)	75/22	85/13	85/13	79/18
$\overline{W_{R_{1st/2nd}}}$ (%)	65/23	67/15	67/14	68/20
$\overline{W_{T_{1st/2nd}}}$ (%)	9/1	15/2	15/2	10/1
$\overline{\Delta U}_{1st/2nd}$[d] (%)	1/−2	3/−4	3/−3	1/−3
$\overline{W_{C_{AH/DH}}}$[e] (%)	45/30	56/29	46/39	45/35
$\overline{W_{R_{AH/DH}}}$ (%)	32/32	33/32	27/40	32/37
$\overline{W_{T_{AH/DH}}}$ (%)	8/1	15/1	12/3	8/2
$\overline{\Delta U}_{AH/DH}$[d] (%)	5/−3	8/−4	7/−4	5/−4

[a]While the work $\overline{W_C}$ on the central excited molecule has plateaued by 1 ps (see Figure 3), the values of its various contributions given by eq 9 are stabilized by 2 ps, which has determined this choice for the values in the table. [b]Time-dependent, spatially independent electric field excitation with a carrier frequency of 700 cm^{-1}. [c]First and second hydration shells. [d]The negative sign indicates that $\overline{\Delta U}$ is negative. [e]AH (molecules accepting H-bonds from the central water), DH (molecules donating H-bonds to the central water). Since these are first hydration shell waters (see Figure 1a), the percentages given, e.g., for $\overline{W_{C_{AH/DH}}}$, in the *x*-axis excitation case, sum (within error bars) to the first hydration shell value in $\overline{W_{C_{1st/2nd}}}$ in the *x*-axis column. The same relation applies to $\overline{W_{R_{AH/DH}}}$ and the first hydration shell value in $\overline{W_{R_{1st/2nd}}}$, etc.

among rotational modes. A better understanding of this interplay requires the analysis of the dependence on distance from the excited molecule, and will be undertaken in the following section. We will focus for the remainder of this section on the features of Figure 3.

We note first that the dominance of transfer into rotation is also consistent with the conclusions of Saito and co-workers.[26] In their approach, the whole sample is excited, and from the dynamics of total excess energies (rotational, translational, and potential), a phenomenological model is fitted. The role of transfer into rotation is inferred from the lifetimes of each assumed process. Indeed, they turn out to be similar to those of a similar model in ref 5 for the bend relaxation process, the forerunner to the quantitative analysis in ref 6, where similar conclusions regarding the role of transfer into rotation were proposed. In addition, these authors[26] also infer a slow increase of excess translational energy of the entire sample, again in good accord with those found in ref 4 and the present results.

Proceeding with our analysis, we can note that the time interval in which the changes are most pronounced in Figure 3 is from 0 to 0.1 ps. For $t \sim 2$ ps, all the terms have reached asymptotically stable values, with the magnitude of the work on the excited water molecule rotation $|\overline{W_C}|$, which is the absolute value of the molecule's rotational kinetic energy loss, having plateaued long before this.[38] The first significant variation of $|\overline{W_C}|$, within the first ∼15 fs, is a decrease in the central water's rotational kinetic energy, in agreement with the sharp decrease in the excited water's rotational kinetic energy for the three NEMD trajectories in Figure 2a within the same interval. This decrease is clearly due to a corresponding increase in $\overline{\Delta U}$, the potential energy of its interaction with the remaining "solvent" water molecules. This conversion is of course expected, since

dx.doi.org/10.1021/jp308648u | J. Phys. Chem. B 2013, 117, 4541−4552

the network of intermolecular H-bonds is distorted—strain is created—when the central molecule starts to rotate more intensely.

In a feature related to the average rotational kinetic energy in Figure 2b, Figure 3 shows that, at time $t \sim 15$ fs, both $|\overline{W_C}|$ and $\overline{\Delta U}$ exhibit an oscillatory character. The rotation with respect to the x-axis is, on average, reversed due to the repulsive torques from the distorted network of H-bonds (the rotational caging described above), and the molecule begins a "backward" rotation with respect to the principal x-axis, reducing the repulsion (see also Appendix B). Hence, the rotational kinetic energy of the central molecule transiently increases and decreases in the time interval of ~15−35 fs due to a decrease and increase in the interaction potential energy due to the completion of the cage oscillation. After this interval, any coherence is largely lost, and the central water's rotational kinetic energy decreases as does the potential energy.

Turning our attention now to the surrounding water molecules, the work on their translational and rotational degrees of freedom in Figure 3 starts to build up significantly after ~10 fs, and is dominated by the work on rotation. This slight time delay with respect to the buildup of potential energy, also seen in ref 4, is readily understood: the only path for energy transfer between the molecules is via the intermolecular interactions, i.e., the intermolecular forces and torques deriving from the potential energy and associated with the "strain" created in the environment of the excited water. An additional marked feature in Figure 3 concerning the solvent water pickup of kinetic energy is the slight pause in the steady increase in the solvent rotational kinetic energy, in the midst of the rotational cage oscillation (which may be related to the partial restoration of the excited water's initial rotational kinetic energy), after which there is an incoherent increase of this energy. It is also to be noted that there is a feeble transient for translational kinetic energy of the central molecule. Since there is no direct coupling between rotation and translation of the initially rotationally excited central molecule, this buildup represents a follow-up process of the initial flux from the central molecule into potential energy, an excess translational energy which gets finally transferred into the solvent motions.

Keeping our attention on translational energy, we end this section by addressing the transfer of energy into translational degrees of freedom within the hydration shell (~10% of the total energy). It results from the computation of the sum in eq 10, and therefore, in this case, it is not a secondary process but a direct flux that draws rotational energy from the excited molecule and transfers it into translations of its neighbors. It might represent a difference from the phenomenological model in ref 26, in which translational energy buildup seems to constitute the last link in a cascade mechanism, in which energy trickles down from high frequency to low frequency rotational modes and from these into translational modes. We see here that, while direct rotation to translation transfer is inefficient, a direct transfer takes place (of course this does not preclude the existence of additional pathways, i.e., a simultaneous detour through lower frequency librations). This transfer, as will be shown, is robust in terms of variations of initial excitation energy, excited axis, temperature, and excitation procedure (including variations of the librational frequency initially excited).

4.3. Hydration Shell Analysis. In the preceding, we have established that the energy flow for the librational relaxation is strongly dominated by the transfer to the rotational degrees of freedom of the water molecules surrounding the excited water molecule. Equally important, the power and work approach allows as well to study the dependence of the energy transfer on the distance from the central molecule.

We first examine the energy transfer in terms of the excited water molecule's hydration shells, irrespective of the modes involved. The contributions from the first shell, the second shell, and the remainder of the solvent to the work on the rotational degrees of freedom $|\overline{W_C}|$ of the central excited molecule (magnitude of the rotational energy loss) are shown in Figure 4a (see also fourth entry in Table 1). It turns out that

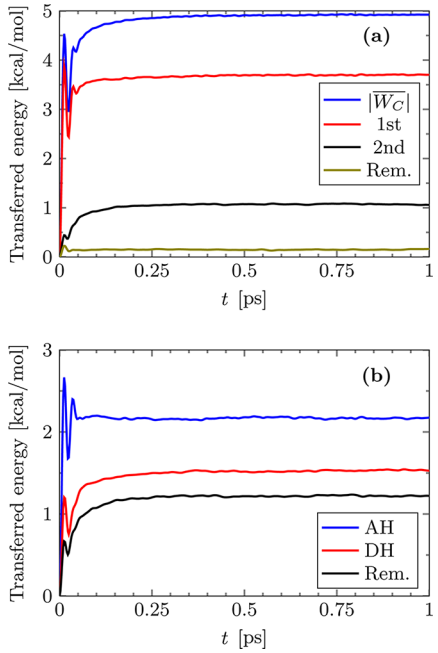

Figure 4. (a) The magnitude of the nonequilibrium average work $|\overline{W_C}|$ on the central water molecule, the work contribution from the first hydration shell water molecules, the work contribution from the second hydration shell water molecules, and the work contribution from the remaining water molecules (Rem.). (b) The work contribution from the molecules accepting H-bonds (AH), the work contribution from the molecules donating H-bonds (DH), and the work contribution from the, remaining, water molecules (Rem.). Note that AH and DH waters are by definition first shell waters; see Figure 1a.

the process is highly local: the first shell, second shell, and remaining contributions are approximately 75, 22, and 3%, respectively, for x-axis excitation, with even higher first shell dominance for the remaining axis excitations (see Table 1 entries $\overline{W_{C_{1st/2nd}}}$). A similar conclusion was also reached by Rey and Hynes for the different case of water bend vibrational relaxation,[6] with the respective contributions being approximately 62, 33, and 5%. The relative weight of first and second shell contributions is slightly different in this case, with a somewhat lesser contribution of the first shell but with almost exactly the same overall transfer into first plus second shell. One might speculate on the transfer being slightly less local (62% to first shell for bend relaxation, compared to 75% in the present work). As has already been stressed, bend relaxation is a process for which the main component is a transfer into self-rotation, followed by a transfer into the immediate neighbors, and in this sense, it is similar to the simpler process studied

dx.doi.org/10.1021/jp308648u | J. Phys. Chem. B 2013, 117, 4541−4552

here. In addition, there is a channel in which energy goes directly from the bend into the surrounding molecules, and for which the percentages are closer to the ones found here (~70% of the work on the vibrational mode is performed by first shell molecules).[5] While being lower than the 75% found here, it is clear that only part of the difference can be assigned to this pathway. We must conclude that rotation to rotation transfer is somewhat less efficient during bend relaxation than for pure rotational relaxation (present work). The difference should probably be ascribed to the different dynamics of a molecule with both vibrational and rotational excitation as compared to a molecule with only rotational excitation (the possible effect of how the molecule got rotationally excited does not seem relevant, as the results are largely unaffected by the excitation method used; see below). Finally, we remark how the present methodology is able to easily uncover the local nature of the process, an important feature that is missed in approaches that focus solely on excess energies.

Since energy transfer to the first hydration shell was just shown to be dominant, it is interesting to determine how this work contribution is distributed among the hydrogen-bonded molecules. To this end, Figure 4b displays the work contributions from the water molecules accepting H-bonds from the rotationally excited water (AH, molecules 1 and 2 in Figure 1a), the work contribution from those molecules donating H-bonds (DH, molecules 3 and 4 in Figure 1a), and the work contribution from all other water molecules (which, from Figure 4a, are primarily in the second hydration shell and beyond). The new information gained is that the energy transfer to water molecules accepting H-bonds dominates over energy transfer to H-bond donating waters for all excitations, albeit with varying proportions as indicated by the $\overline{W}_{C_{AH/DH}}$ entries of Table 1: the ratio being 1.5, 1.9, and 1.2 for the *x*-, *y*-, and *z*-axis excitations, respectively.[39] As for the reasons for this dominance, in general terms, the displacements of the hydrogens within the central molecule will, for all initial rotations, be larger than that of the oxygen and therefore molecules accepting hydrogen bonds will be the more perturbed in principle. It must be said though that this kind of reasoning is to be used with caution. It suffices to say that in the case of bend relaxation it is found[5] that work done by AH molecules on the central molecule rotation is about half of that performed by DH molecules, i.e., the other way around from the present case. As was argued previously when discussing the slightly different weights between first and second shell participation, this reinforces the notion that, despite their evident similarities (locality, overwhelming transfer into rotations), pure rotational relaxation cannot be exactly assimilated to rotational energy transfer during bend relaxation. The larger amplitude of bend vibration in this case evidently perturbs the dynamics of rotational energy transfer, which is reflected in a varying role of first/second shells and AH/DH molecules within the first shell.

It remains to connect these results for the distance dependence of energy transfer with the previously established (Figure 3 for *x*-axis excitation) dominance of transfer to the rotation over that to translation of the water molecules surrounding the central water. From the $\overline{W}_{R_{1st/2nd}}$ and $\overline{W}_{T_{1st/2nd}}$ values, rotation dominates over translation, in the contributing fractions 65/75 vs 9/75 in the first shell and 23/22 vs 1/22 in the second shell. Besides the known dominance of transfer to the first shell, we learn that all transfer into translations is directed toward first shell molecules, i.e., toward molecules in direct contact with the initially excited one. A very similar result was obtained in the case of the bend relaxation[6] for transfer into translational motion. In consequence, translational energy transfer is more local than rotational energy transfer, and the latter is in turn more local than vibrational energy transfer. Summing up the previous considerations, we might construct a highly simplified picture on the basis that rotational energy is transferred mostly to immediate neighbors' rotations and, at each "transfer", about 10−15% of the energy is lost locally in the form of translational energy. Although we have not pursued this pathway here, it might be interesting to construct a kinetic model for the spatial dissipation of the initial energy on the basis of these simple tenets, as it might help aid in understanding the subsequent stages of thermalization of the solvent molecules.

We will now narrow the analysis to the AH and DH molecules and their rotational/translational mode participation. We ask how the rotational/translational energy acceptance is connected to the H-bond-accepting or -donating character of the first shell waters (see final cluster of values in Table 1's first column). From the $\overline{W}_{R_{AH/DH}}$ and $\overline{W}_{T_{AH/DH}}$ values, we see by a vertical comparison that both the H-bond acceptors and donors are preferentially rotationally, rather than translationally, excited by energy transfer from the excited water molecule: for the AH waters in the ratio 32/8 and for the DH waters in the ratio 32/1. These results indicate that the AH waters are noticeably more effective than the DH waters in the minority component translational excitation. Such a substantial difference can be explained again in terms of the mechanical view according to which the hydrogens undergo larger displacements, and hence the H-bonds are distorted to a large extent for the molecules accepting H-bonds, so that they have to translate accordingly.

There are additional issues worth noticing related with the AH and DH molecules participation, connected with translational and potential energy. From the final entry in Table 1, we see that potential energy has not attained full equilibrium by the end of the NEMD trajectories. Actually, potential energy is still slightly higher than the equilibrium one for the first shell and, to a lesser extent, the opposite scenario holds for the second shell. We see that structural relaxation has not been completed yet, what should be expected given the hindered nature of librations previously discussed: kinetic and structural aspects go hand in hand during the relaxation process (structural nonequilibrium has also been noticed in ref 26). As a consequence of the imbalance of transfer to translations discussed in the previous paragraph, together with the nonequilibrium for potential energy just mentioned, we find that work on rotations of AH and DH molecules turns out to be fairly symmetric (32/32 ratio in Table 1). We finally note that the fact that AH and DH molecules behave differently with respect to the rotational energy transfer from the central molecule indicates that the designation of either AH or DH to a solvent molecule is meaningful on the time scale of the energy transfer, which is in compliance with the relatively long hydrogen-bond lifetime (as compared to the time scale of the energy transfer) of 700−800 fs.[40]

The above considerations challenge the simple intuition one might have according to which, given a pair of molecules (say A and B), the work that A exerts on rotation of B equals minus the work of B on rotation of A. Although what follows is just a simple corollary of the formulas in section 2 and Appendix A, it

dx.doi.org/10.1021/jp308648u | J. Phys. Chem. B 2013, 117, 4541−4552

might be worth some short elaboration. Of course, what actually holds is similar to the above statement but for the total work plus interaction energy. It might prove useful to stress the relationship of the work done *on* the central water (W_C) and the work done *by* that water on a neighbor (W_T, W_R). We start for instance from the basic relation given in eq A-4. After summing over all the atoms on each molecule and integrating, we get

$$W_C = -\Delta U - W_T - W_R \tag{12}$$

When the potential energy change contribution is small (it usually tends to zero as time grows), it can be ignored so that we can write approximately

$$W_C = -W_T - W_R \tag{13}$$

which shows that, while W_C only consists (on the average) of rotational work on the central molecule, it equals minus the sum of translational and rotational work of the central molecule on its neighbor; i.e., and as it should be, rotational energy is transferred into a mixture of translational and rotational energy of its neighbor. Turning to the case that originated this discussion, while it is true that AH molecules dominate DH molecules regarding the work they perform on the central molecule (by a proportion 45/30), this is perfectly compatible (and in fact complementary) with a balance (32/32 ratio) of the work of the central molecule on rotation of AH and DH molecules. A very similar scenario occurs for bend relaxation[6] in which, as stated above, DH molecules dominate AH molecules in the work they perform on the central molecule rotation, while the work that the relaxing molecule does on their rotational motion is almost balanced as in the present case.

4.4. Energy and Temperature Dependence. We now turn to an investigation of the dependence of the rotational relaxation on the excitation energy and the temperature. Figure 5a displays the normalized excess rotational kinetic energy, $\overline{R}(t) - \langle R \rangle$, of the central water molecule for four different excitation energies, with all the excitations with respect to the x-axis. The very initial decay to ~0.1 remains very nearly the same in each case. The later timer behavior is however energy-dependent, and reflects the decreasing coherence as the excitation energy is increased and the role of the restoring torque is evidently diminished. Thus, the excitation energy affects both the position and amplitude of the first local maximum, the former being shifted to slightly longer times and the latter decreasing somewhat as the energy increases. It is however striking that the coherence persists up to such high excitation energies. A further effect reflecting the decreasing rotational coherence is that the second local maximum, which is a more subtle aspect of the coherence, vanishes for the largest excitation energies 10−15 kcal/mol. On the other hand, the long-time, i.e., post ~50 fs, behavior of the decay of the rotational kinetic energy is not significantly affected by the level of initial excitation. A final and important point is that, for all the excitation energies considered, we find that ~85−90% of the excess rotational kinetic energy is transferred to the rotational degrees of freedom of the solvent waters. This feature indicates that the energy pathway discussed in the previous sections is approximately independent of the excitation energy, a result that we have confirmed by calculations analogous to the lower energy results in Figure 3.

The normalized excess rotational kinetic energy of the central molecule for three different temperatures is shown in Figure 5b for the 1 kcal/mol excess rotational energy case. In view of the robust character of the primary coherent oscillation effects *vis a vis* the excitation energy variation in Figure 5a, we do not anticipate, and do not find, marked temperature effects. The positions of the local extrema are not affected by the temperature, but their amplitudes and the degree of rotational coherence are decreased slightly. As anticipated, the very modest magnitudes of the temperature effects here are consistent with the much smaller magnitude of initial water rotational kinetic energy compared to the three higher energy excitation situations in Figure 5a.

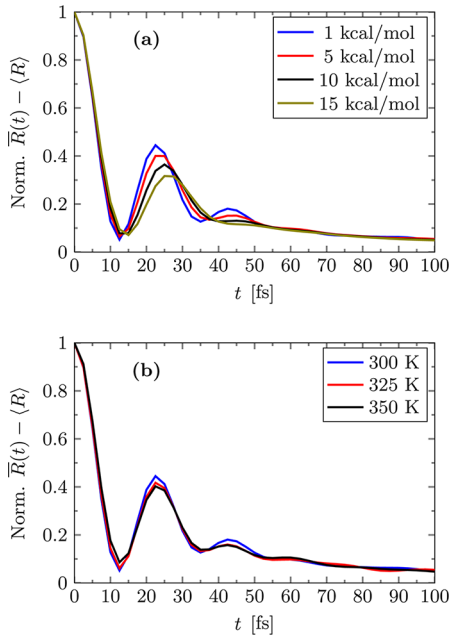

Figure 5. (a) Normalized nonequilibrium average excess rotational kinetic energy of the central water molecule for four different excitation energies. The instantaneous excitation is with respect to the principal x-axis. (b) Normalized nonequilibrium average excess rotational kinetic energy for three different temperatures, where the 1 kcal/mol instantaneous excitation of the central water is with respect to the principal x-axis.

Finally, these general features of the x-axis excitation results are largely axis-independent: we show in the Supporting Information that there is a similar dependence on the excitation energy and the temperature for instantaneous excitation with respect to the water molecule y- and z-axes.

4.5. Rotational Excitation via an External Electric Field. Since, as we have seen, the librational relaxation occurs on the time scale of tens of femtoseconds, the width of the experimental optical excitation pulse could certainly influence aspects of the relaxation. In order to explore this issue, we compare some of our instantaneous excitation results with a rotational excitation carried out by coupling the point charges of the central water molecule to a linear polarized time-dependent electric field with no spatial dependence across the molecule.[41] This coupling is introduced by adding the term $-\boldsymbol{\mu}\cdot\mathbf{E}(t)$ to the Hamiltonian, where $\boldsymbol{\mu}$ is the dipole moment of the central water and $\mathbf{E}(t)$ is the time-dependent electric field. The electric field is taken to have a Gaussian shape with fwhm = 50 fs, and is centered at t = 100 fs. The carrier frequency of the pulse is ν = 700 cm^{-1}, and the intensity is $I_0 = 1.0 \times 10^{13}$ W/cm^2. Since the intensity is proportional to the maximum electric field amplitude squared E_0^2, the strength of the coupling term, and thereby the excitation energy, is dependent on the

dx.doi.org/10.1021/jp308648u | J. Phys. Chem. B 2013, 117, 4541−4552

intensity. We have adjusted the field intensity so that the excitation energy is on average ∼5 kcal/mol for our selected example. The 700 cm^{-1} carrier frequency of the pulse approximately corresponds to the peak in the liquid water librational frequency spectrum,[3] which is shown in Figure 6.

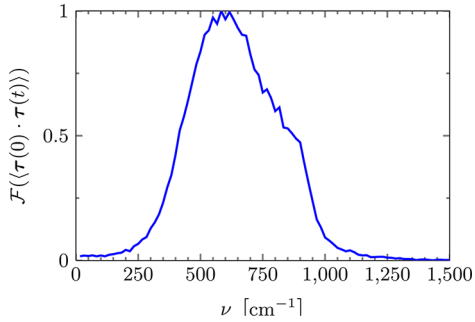

Figure 6. The Fourier transform of the normalized equilibrium time correlation function for the torque on the central water molecule. This "librational band" has a peak at $\nu \approx 650$ cm^{-1}.

Before proceeding, we pause to note an approximate connection of the spectral peak with the rotational caging illustrated in Figure 2b. The avarage peak there occurs near 25 fs, which in a simple (and approximate) harmonic picture gives a period of 50 fs, corresponding to a spectral peak at 650 cm^{-1}.

The work terms for this time-dependent field excitation are plotted in Figure 7 and should be compared with the

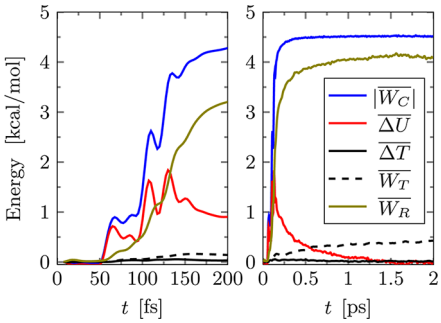

Figure 7. For rotational excitation of the central water with a time-dependent electric field (ν = 700 cm^{-1}), the absolute value of the average nonequilibrium work on the rotational degrees of freedom $|\overline{W_C}|$ of the central molecule, the difference in potential energy $\overline{\Delta U}$ between time 0 and t, the difference in translational kinetic energy $\overline{\Delta T_C}$ of the central water, and the work on the translational $\overline{W_T}$ and the rotational degrees of freedom $\overline{W_R}$ of the water solvent.

instantaneous excitation results in Figure 3. Clearly, the time dependence of these terms during the first few hundred fs of the simulations differs for the instantaneous and time-dependent excitations, as is to be expected given the different mechanisms and time scales of the short time angular momentum alteration. However, their long-time behavior is very much alike. For example, in each case, ∼90% of the excited water's excess rotational kinetic energy is transferred to the rotational degrees of freedom of the surrounding solvent waters. Hence, the method of excitation does not affect the relative contributions of the rotationally excited water's energy flow to translational and rotational degrees of freedom of the surrounding water solvent. Indeed, the I_0 column of Table 1 shows the very close correspondence for all quantities calculated for the different excitation methods.

We have also investigated how the characteristics of the librational energy transfer depend on the frequency of the electric field by carrying out simulations with frequencies of 100, 400, 700, 1000, and 1300 cm^{-1}, while keeping the same field intensity. We find that the amount of energy transferred from the electric field to the central water molecule depends strongly on the frequency; $E_{100\ cm^{-1}} \approx 0.4$ kcal/mol, $E_{400\ cm^{-1}} \approx 3.4$ kcal/mol, $E_{700\ cm^{-1}} \approx 4.5$ kcal/mol, $E_{1000\ cm^{-1}} \approx 1.9$ kcal/mol, and $E_{1300\ cm^{-1}} \approx 0.3$ kcal/mol. The peaking of the absorption near 700 cm^{-1} here is in agreement with Figure 6 and the study of Yagasaki and Saito,[26] who examined the IR absorption by coupling the entire system to an electric field (of frequencies 500, 700, and 900 cm^{-1}), as opposed to the single water molecule coupling in the present study.

For all the frequencies examined, we find that ∼85−91% of the excess rotational kinetic energy is transferred to the rotational degrees of freedom of the solvent waters. This result, which is in good agreement with the section 4.4 results for the energy dependence for the librational relaxation subsequent to instantaneous rotational excitation, indicates that the energy flow route is quite robust: its dependence on the electric field carrier frequency (and therefore, on the excitation energy) is very weak.

5. CONCLUDING REMARKS

We have investigated the ultrafast librational relaxation of H_2O in liquid water via classical NEMD simulations, and elucidated the energy flow pattern. The rotational degrees of freedom of the solvent are the primary acceptors of energy; in fact (averaging over the results for the three Cartesian axes), ∼85% of the excess rotational kinetic energy is transferred to the rotational modes, and the rest of the ∼15% is transferred to the translational modes. These results are not affected by the chosen rotational excitation energy of 5 kcal/mol and the temperature of 300 K. Our simulations show that the same behavior of the librational relaxation is maintained for excitation energies up to 15 kcal/mol and temperatures up to 350 K. Furthermore, two excitation methods are used and the results are largely independent of the method. Since the time-scale for the first period of the oscillation in the rotational energy decay corresponds to the time-scale of the reversal of the angular momentum under equilibrium conditions, the reported results are also elucidating the generic librational motion in equilibrated water.

We find that the closest solvent molecules receive most of the energy. The first solvent shell is the primary energy acceptor with (on average) ∼80% of the energy, and the second solvent shell receives the rest, approximately. Furthermore, we conclude that the transfer of energy to rotation of the AH and DH molecules is fairly symmetric, whereas the transfer of energy to translation is highly asymmetric, where the AH molecules dominate. These results are in good agreement with the recent bend vibrational relaxation study by Rey and Hynes.[6]

■ APPENDIX A

Here we present an alternative derivation of our fundamental formula for the power of the rotational kinetic energy; see eq 7. In an isolated system of rigid molecules, the energy E can be partitioned into kinetic energy $K = T + R$ (T denotes translational kinetic energy and R rotational kinetic energy) and

dx.doi.org/10.1021/jp308648u | J. Phys. Chem. B 2013, 117, 4541−4552

potential energy U. As usual, the kinetic energy of molecule i is given by a sum of contributions from each atom α_i

$$K_i = \frac{1}{2}\sum_{\alpha_i} m_{\alpha_i}\mathbf{v}_{\alpha_i}\cdot\mathbf{v}_{\alpha_i} \tag{A-1}$$

The power of the kinetic energy of molecule i reads

$$P_i \equiv \frac{\mathrm{d}K_i}{\mathrm{d}t} = \sum_{\alpha_i}\mathbf{F}_{\alpha_i}\cdot\mathbf{v}_{\alpha_i} \tag{A-2}$$

where $\mathbf{F}_{\alpha_i}$ is the force on atom α_i, which can be partitioned such that

$$P_i = \sum_{\alpha_i}\sum_{j}\sum_{\beta_j}\mathbf{F}_{\alpha_i,\beta_j}\cdot\mathbf{v}_{\alpha_i} \tag{A-3}$$

with $\mathbf{F}_{\alpha_i,\beta_j}$ denoting the force on atom α_i due to the interaction with atom β_j. The term $\mathbf{F}_{\alpha_i,\beta_j}\cdot\mathbf{v}_{\alpha_i}$ is the change in kinetic energy of atom α_i due to the interaction with atom β_j. Since the increase/decrease in kinetic energy is equal to the decrease/increase in potential energy of the isolated system, we can write

$$\mathbf{F}_{\alpha_i,\beta_j}\cdot\mathbf{v}_{\alpha_i} + \mathbf{F}_{\beta_j,\alpha_i}\cdot\mathbf{v}_{\beta_j} = -\frac{\mathrm{d}U_{\alpha_i,\beta_j}}{\mathrm{d}t} \tag{A-4}$$

where U_{α_i,β_j} denotes the potential energy of atom α_i and β_j due to their interaction.[42] In the rigid rotor approximation, the summation over j does not include i, and we obtain

$$P_i = -\sum_{\alpha_i}\sum_{j\neq i}\sum_{\beta_j}\frac{\mathrm{d}U_{\alpha_i,\beta_j}}{\mathrm{d}t} - \sum_{\alpha_i}\sum_{j\neq i}\sum_{\beta_j}\mathbf{F}_{\beta_j,\alpha_i}\cdot\mathbf{v}_{\beta_j} \tag{A-5}$$

We write the velocity vector $\mathbf{v}_{\beta_j}$ as

$$\mathbf{v}_{\beta_j} = \mathbf{v}_j + \omega_j \times \mathbf{r}_{\beta_j} \tag{A-6}$$

where $\mathbf{v}_j$ is the center of mass velocity of molecule j, $\boldsymbol{\omega}_j$ is the angular velocity of molecule j, and $\mathbf{r}_{\beta_j}$ is the position of atom β_j with respect to the center of mass of molecule j. This leads to

$$P_i = -\sum_{j\neq i}\frac{\mathrm{d}U_{i,j}}{\mathrm{d}t} - \sum_{j\neq i}\mathbf{F}_{j,i}\cdot\mathbf{v}_j - \sum_{j\neq i}\boldsymbol{\tau}_{j,i}\cdot\boldsymbol{\omega}_j \tag{A-7}$$

where $\mathbf{F}_{j,i}$ is the force and $\boldsymbol{\tau}_{j,i}$ is the torque on molecule j (with respect to the center of mass) due to the interaction with molecule i. Here, $U_{i,j}$ is the interaction potential energy of molecule i and j. The summations over α_i and β_j have been carried out, i.e., the atoms of each molecule, since we are interested in the contribution to the power from each molecule.

Since the kinetic energy of molecule i is partitioned into translational and rotational contributions

$$P_i = P_i^{\mathrm{T}} + P_i^{\mathrm{R}} = \sum_{j\neq i}\mathbf{F}_{i,j}\cdot\mathbf{v}_i + P_i^{\mathrm{R}} \tag{A-8}$$

we recover eq 7 for the power of the rotational kinetic energy of the ith molecule

$$P_i^{\mathrm{R}} = -\frac{\mathrm{d}U}{\mathrm{d}t} - \frac{\mathrm{d}T_i}{\mathrm{d}t} - \sum_{j\neq i}\mathbf{F}_{j,i}\cdot\mathbf{v}_j - \sum_{j\neq i}\boldsymbol{\tau}_{j,i}\cdot\boldsymbol{\omega}_j \tag{A-9}$$

APPENDIX B

In our discussion in section 4.2 of the work on the excited water molecule rotation, the average rotational kinetic energy of that molecule, and its potential energy of interaction with the remaining waters in Figures 2 and 3, we indicated that the pronounced short time oscillation was associated with rotational caging of the water molecule. Here we present the origin of this statement, extending via a linear response perspective the discussion in ref 4 to a single axis rotational excitation and, in addition, shedding some light on the exchange of energy between the excited and nonexcited axis rotations.

For rotational excitation about the x-axis of the water molecule, the natural linear response comparison between the nonequilibrium decay and the decay of the equilibrium fluctuations is between the normalized nonequilibrium decay

$$\overline{\delta R}(t)/\overline{\delta R}(0) = (\bar{R}(t) - \langle R\rangle)/(\bar{R}(0) - \langle R\rangle) \tag{B-1}$$

and the normalized equilibrium time correlation function (tcf) involving the fluctuations of the x-axis and the full rotational kinetic energies

$$\langle \delta R_x(0)\delta R(t)\rangle / \langle \delta R_x(0)\delta R(0)\rangle \tag{B-2}$$

Figure 8 shows that the agreement between these two functions is excellent for 1 kcal/mol excitation (i.e., in the thermal range) and only slightly less satisfactory, mainly beyond the first oscillation peak, for the 5 kcal/mol excitation (we comment on higher excitation energies in section 4.4).

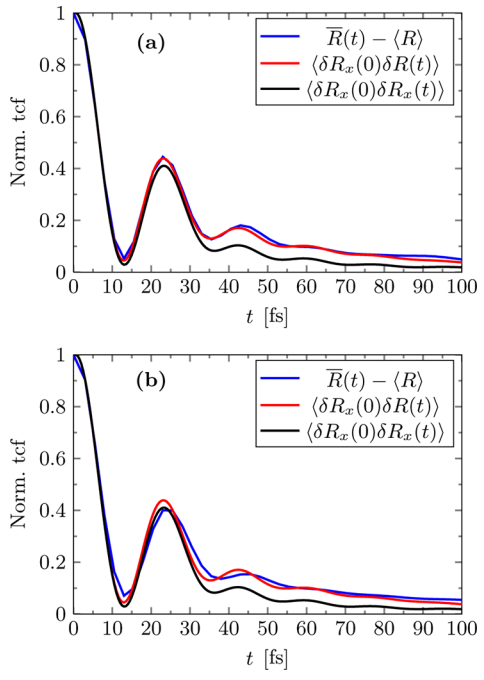

Figure 8. Comparison of the nonequilibrium rotational kinetic energy dissipation $\bar{R}(t) - \langle R\rangle$ for the central molecule and the equilibrium time correlation functions $\langle \delta R_x(0)\delta R(t)\rangle$ and $\langle \delta R_x(0)\delta R_x(t)\rangle$. The nonequilibrium function and each tcf are normalized by their respective initial values. (a) 1 kcal/mol instantaneous excitation with respect to the principal x-axis. (b) 5 kcal/mol instantaneous excitation with respect to the principal x-axis.

Figure 8 also includes a comparison with the exclusively x-axis normalized tcf

$$\langle \delta R_x(0)\delta R_x(t)\rangle / \langle \delta R_x(0)\delta R_x(0)\rangle \tag{B-3}$$

dx.doi.org/10.1021/jp308648u | J. Phys. Chem. B 2013, 117, 4541−4552

The first use of this last comparison is to gain an impression of the exchange of rotational kinetic energy between rotation about the x-axis and the remaining y- and z-axes. The difference between eqs B-2 and B-3 in Figure 8—which is zero if there is no exchange—indicates that, in the equilibrium ensemble, the exchange sets in primarily just past the oscillation peak, and is not negligible, providing up to about a factor of 2 in the correlations at these longer times.

The second use of the comparison, given the good agreement between the nonequilibrium function and both equilibrium functions up to and including the neighborhood of the first oscillation peak, is that we can use the x-axis tcf in eq B-3 to demonstrate the peak's origin in the rotational caging, as follows. If the statistical behavior of the x-axis angular momentum J_x dynamics is Gaussian, then it is straightforward to show that the behavior of the x-axis tcf in eq B-3 is related to the square of the normalized tcf of J_x by

$$\langle \delta R_x(0)\delta R_x(t)\rangle / \langle [\delta R_x]^2\rangle = \langle \delta {J_x}^2(0)\delta {J_x}^2(t)\rangle / \langle [\delta J_x(0)]^2\rangle = [\langle J_x(0)J_x(t)\rangle / \langle {J_x}^2\rangle]^2 \quad \text{(B-4)}$$

where we have canceled out factors involving the x moment of inertia and exploited the Gaussian behavior in the last member. Figure 9 shows the first minimum in the normalized J_x tcf,

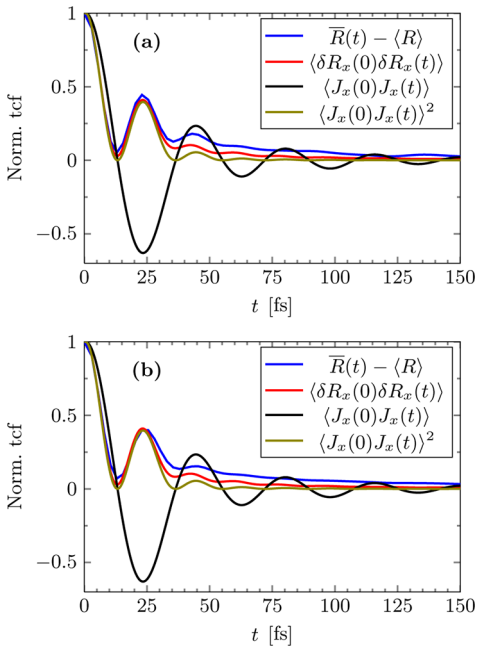

Figure 9. Comparison of the nonequilibrium rotational kinetic energy dissipation $\overline{R}(t) - \langle R\rangle$ for the central molecule and the equilibrium time correlation functions $\langle \delta R_x(0)\delta R_x(t)\rangle$, $\langle J_x(0)J_x(t)\rangle$, and $\langle J_x(0)J_x(t)\rangle^2$. The nonequilibrium function and each tcf are normalized by their respective initial values. (a) 1 kcal/mol instantaneous excitation with respect to the principal x-axis. (b) 5 kcal/mol instantaneous excitation with respect to the principal x-axis.

signaling the rotational caging reversal of the sign of the initial angular momentum. The figure also shows that this reversal produces an oscillation peak in the square of the J_x tcf, which is in quite good agreement with the peak in the δR_x tcf and—most importantly—in the nonequilibrium relaxation of the rotational kinetic energy for both the 1 and 5 kcal/mol excitations. (The demonstration of the same conclusion for the y- and z-axis excitations is provided in the Supporting Information.) While the agreement clearly deteriorates subsequently, due to exchange of different axes' rotational kinetic energy and the breakdown of the Gaussian assumption, there nonetheless remains a reasonable identification of the second, muted peak in the nonequilibrium decay with a subsequent reversal of angular momentum.

■ ASSOCIATED CONTENT

Supporting Information

The y- and z-axes excitation results complementary to the x-axis excitation material in section 4.4 and Appendix B of the text. This material is available free of charge via the Internet at http://pubs.acs.org.

■ AUTHOR INFORMATION

Corresponding Author

*E-mail: klaus.moller@kemi.dtu.dk (K.B.M.); rosendo.rey@upc.edu (R.R.); james.hynes@colorado.edu (J.T.H.).

Notes

The authors declare no competing financial interest.

■ ACKNOWLEDGMENTS

This work was supported by the Niels Bohr Foundation (J.P.), the Danish National Research Foundation (J.P. and K.B.M.), M.C.I. FIS2009-13641-C02-01 and D.G.R. 2009GR-1003 (R.R.), and by NSF grant CHE-1112564 (J.T.H.). J.T.H. expresses on this occasion his deep appreciation for the many contributions of Paul Barbara.

■ REFERENCES

(1) Huse, N.; Ashihara, S.; Nibbering, E. T. J.; Elsaesser, T. *Chem. Phys. Lett.* **2005**, *404*, 389−393.
(2) Ashihara, S.; Huse, N.; Espagne, A.; Nibbering, E. T. J.; Elsaesser, T. *Chem. Phys. Lett.* **2006**, *424*, 66−70.
(3) Ashihara, S.; Huse, N.; Espagne, A.; Nibbering, E. T. J.; Elsaesser, T. *J. Phys. Chem. A* **2007**, *111*, 743−746.
(4) Ingrosso, F.; Rey, R.; Elsaesser, T.; Hynes, J. T. *J. Phys. Chem. A* **2009**, *113*, 6657−6665.
(5) Rey, R.; Ingrosso, F.; Elsaesser, T.; Hynes, J. T. *J. Phys. Chem. A* **2009**, *113*, 8949−8962.
(6) Rey, R.; Hynes, J. T. *Phys. Chem. Chem. Phys.* **2012**, *14*, 6332−6342.
(7) Pakoulev, A.; Wang, Z.; Dlott, D. D. *Chem. Phys. Lett.* **2003**, *371*, 594−600.
(8) Deàk, J. C.; Rhea, S. T.; Iwaki, L. K.; Dlott, D. D. *J. Phys. Chem. A* **2000**, *104*, 4866−4875.
(9) Lindner, J.; Vöhringer, P.; Pshenichnikov, M. S.; Cringus, D.; Wiersma, D. A.; Mostovoy, M. *Chem. Phys. Lett.* **2006**, *421*, 329−333.
(10) Lindner, J.; Cringus, D.; Pshenichnikov, M. S.; Vöhringer, P. *Chem. Phys.* **2007**, *341*, 326−335.
(11) Rey, R.; Hynes, J. T. *J. Chem. Phys.* **1996**, *104*, 2356−2368.
(12) Rey, R.; Møller, K. B.; Hynes, J. T. *Chem. Rev.* **2004**, *104*, 1915−1928.
(13) Lawrence, C. P.; Skinner, J. L. *J. Chem. Phys.* **2002**, *117*, 5827−5838.
(14) Whitnell, R. M.; Wilson, K. R.; Hynes, J. T. *J. Phys. Chem.* **1990**, *94*, 8625−8628.
(15) Whitnell, R. M.; Wilson, K. R.; Hynes, J. T. *J. Chem. Phys.* **1992**, *96*, 5354−5369.
(16) Laage, D.; Hynes, J. T. *J. Phys. Chem. B* **2008**, *112*, 14230−14242.
(17) Stillinger, F. H. *Science* **1980**, *209*, 451−457.

(18) (a) Reid, P. J.; Silva, C.; Walhout, P. K.; Barbara, P. F. *Chem. Phys. Lett.* **1994**, *228*, 658−664. (b) Silva, C.; Walhout, P.; Yokoyama, K.; Barbara, P. *Phys. Rev. Lett.* **1998**, *80*, 1086−1089.
(19) (a) Schwartz, B. J.; Bittner, E. R.; Prezhdo, O. V.; Rossky, P. J. *J. Chem. Phys.* **1996**, *104*, 5942−5955. (b) Prezhdo, O. V.; Rossky, P. J. *J. Phys. Chem.* **1996**, *100*, 17094−17102. (c) Schwartz, B. J.; Rossky, P. J. *J. Chem. Phys.* **1996**, *105*, 6997−7010.
(20) Gertner, B. J.; Whitnell, R. M.; Wilson, K. R.; Hynes, J. T. *J. Am. Chem. Soc.* **1991**, *113*, 74−87.
(21) Heidelbach, C.; Schroeder, J.; Schwarzer, D.; Vikhrenko, V. S. *Chem. Phys. Lett.* **1998**, *291*, 333−340.
(22) Vikhrenko, V. S.; Heidelbach, C.; Schwarzer, D.; Nemtsov, V. B.; Schroeder, J. *J. Chem. Phys.* **1999**, *110*, 5273−5285.
(23) Kandratsenka, A.; Schroeder, J.; Schwarzer, D.; Vikhrenko, V. S. *J. Chem. Phys.* **2009**, *130*, 174507.
(24) Yagasaki, T.; Saito, S. *J. Chem. Phys.* **2008**, *128*, 154521.
(25) Yagasaki, T.; Ono, J.; Saito, S. *J. Chem. Phys.* **2009**, *131*, 164511.
(26) Yagasaki, T.; Saito, S. *J. Chem. Phys.* **2011**, *134*, 184503.
(27) Swope, W. C.; Andersen, H. C.; Berens, P. H.; Wilson, K. R. *J. Chem. Phys.* **1982**, *76*, 637−649.
(28) Berendsen, H. J. C.; Grigera, J. R.; Straatsma, T. P. *J. Phys. Chem.* **1987**, *91*, 6269−6271.
(29) Kell, G. S. *J. Chem. Eng. Data* **1975**, *20*, 97−105.
(30) de Leeuw, S. W.; Perram, J. W.; Smith, E. R. *Proc. R. Soc. London, Ser. A* **1980**, *373*, 27−56.
(31) Andersen, H. C. *J. Chem. Phys.* **1980**, *72*, 2384−2393.
(32) (a) Nose, S. *Mol. Phys.* **1984**, *52*, 255−268. (b) Hoover, W. G. *Phys. Rev. A* **1985**, *31*, 1695−1697.
(33) Allen, M. P.; Tildesley, D. J. *Computer Simulation of Liquids*; Oxford University Press: Oxford, 1987.
(34) The standard deviations of the temperature fluctuations are ∼10 and ∼11 K for $T \approx 325$ K and $T \approx 350$ K, respectively.
(35) In the excitation method used in ref 4, the central water molecule is given an excess rotational kinetic energy, e.g., 5 kcal/mol. Therefore, the initial rotational kinetic energy is the excitation energy plus the equilibrium value.
(36) We observe that the time location of the first peaks in Figure 2c does not come in order of increasing moments of inertia, and that the peaks have different heights (i.e., the friction is direction-dependent). Since this order would be obeyed if the effective anharmonic potentials in which the central molecule librates were assumed to be the same for all three directions (if the peak heights were identical), the effective potentials most likely differ for the three rotation directions. This is not surprising when one considers the H-bonding in Figure 1a.
(37) Keutsch, F. N.; Fellers, R. S.; Brown, M. G.; Viant, M. R.; Petersen, P. B.; Saykally, R. J. *J. Am. Chem. Soc.* **2001**, *123*, 5938−5941.
(38) Eventually, 1/3 of the total excess rotational kinetic energy of the central molecule (i.e., ca. 1.7 out of 5 kcal/mol) will end up in translational degrees of freedom (assuming that the excess energy is evenly distributed as potential, translational kinetic, and rotational kinetic energy when the system is completely equilibrated). The black dashed curve, $\overline{W}_T$, in Figure 3 shows that ca. 0.5 kcal/mol of the total excess rotational kinetic energy of the central molecule is transferred directly into translational degrees of freedom of the surroundings. Thus, the remaining ca. 1.2 kcal/mol that eventually ends up in translational degrees of freedom must get there indirectly by intermolecular rotational to translational energy conversion in the surroundings. Likewise, the small rise and fall of the central molecule's translational energy (black curve, $\overline{\Delta T_C}$) is a result of the central molecule being pushed around by the solvent molecules.
(39) As a consistency check of the implementation of the work formula, $\overline{W}_{C_{1st/2nd}}$ and $\overline{W}_{C_{AH/DH}}$ are calculated using both eqs 3 and 7 inserted into eq 8 with identical results.
(40) Møller, K. B.; Rey, R.; Hynes, J. T. *J. Phys. Chem. A* **2004**, *108*, 1275−1289.
(41) For the two excitation methods used in this study, the excitation probablity corresponds to ∼0.5% (1 out of 216 molecules is excited), which matches the experimental energy absorption rate estimated in ref 3.
(42) Thornton, S. T.; Marion, J. B. *Classical Dynamics of Particles and Systems*; Brooks/Cole: Belmont, 2004.